



Düzce University Journal of Science & Technology

Research Article

Numerical Determination Of Cooling Performance On Heat Sink Using Impingement Jet

 Altuğ KARABEY ^{a,*},  Rami Abdulraheem Abdulrazzaq AL-ANI ^b

^a Department of Mechanical Engineering, Faculty of Engineering, Van Yüzüncü Yıl University, Van, TURKEY

^b Department of Mechanical Engineering, Institute of Naturel and Applied Science, Van Yüzüncü Yıl University, Van, TURKEY

* Corresponding author's e-mail address: akarabey@yyu.edu.tr

DOI: 10.29130/dubited.1076314

ABSTRACT

The use of impingement jet technics drew significant attention of researchers in the recent period. In this method, significant heat transfer rates are achieved. The present study examined the cooling performance of the fin pairs, which are aligned in a consecutively enlarging-contracting pattern and have a rectangular geometry, on a heat sink. The target geometry was optimized in the previous study by using the Taguchi method with single nozzle impingement cooling jet. The analyses were performed using four different impingement jet velocities (10, 12, 14, and 16 m/sec.), three different nozzle diameters ($D=50, 63, \text{ and } 75 \text{ mm}$), three different heat flux values ($q=2222, 3333, \text{ and } 4444 \text{ W/m}^2$), and constant nozzle-to-target distance ($h/d=1$) were analyzed. These results were simulated numerically by using the ANSYS Fluent software. The $k-\epsilon$ realizable turbulence model was selected as the best model. The numerical results showed that the mean Nusselt number is directly proportional to the increase in the Reynolds number. The Nusselt number also increased with the increasing nozzle diameter value. The results are illustrated graphically ($Nu-Re$) in the present study. The peak value of the local Nusselt number was found to be at the stagnation point.

Keywords: Ansys Fluent, CFD, Heat sink, Heat transfer enhancement, Impingement jet.

Isı Alıcı Üzerinde Çarpan Jetle Soğutma Performansının Sayısal Olarak Belirlenmesi

ÖZET

Çarpan jet akışına ait tekniklerin kullanımı, son zamanlarda birçok araştırmacı için büyük önem taşımaktadır. Bu yöntem sayesinde, büyük ısı transfer oranları elde edilmektedir. Bu çalışmada, ardışık olarak daralan-genişleyen düzende dizilmiş dikdörtgen geometriye sahip kanatçık çiftlerinin bir ısı alıcı üzerindeki soğutma performansı incelenmiştir. Çalışmada, daha önceden Taguchi yöntemi ile tek nozul sisteminde optimize edilmiş ısı alıcı kullanılmıştır. Analizler, üç farklı lüle çapında ($D=50, 63, 75 \text{ mm}$), üç farklı ısı akısında ($q=2222, 3333, 4444 \text{ W/m}^2$) ve dört farklı jet hızında (10, 12, 14, 16 m/sn), sabit lüle-ısı alıcı mesafesinde ($h/d=1$) gerçekleştirilmiştir. Çalışma, ANSYS Fluent yazılımı kullanılarak sayısal olarak analiz edilmiştir. Analize en uygun model olarak $k-\epsilon$ türbülans modeli seçilmiştir. Sayısal sonuçlar, ortalama Nusselt sayısının Reynolds sayısındaki artışla doğru orantılı olduğunu göstermiştir. Ayrıca Nusselt sayısı, lüle çapı arttıkça artmıştır. Sonuçlar grafiksel olarak ($Nu-Re$) açıklanmıştır. Yerel Nusselt sayısına ait maksimum noktanın jetin durma noktasında olduğu tespit edilmiştir.

Anahtar Kelimeler: Ansys Fluent, CFD, Isı alıcı, Isı transferinin iyileştirilmesi, Çarpan jet.

I. INTRODUCTION

Offering a higher heat transfer performance, jet impingement technology draws gradually increasing attention in engineering studies. Thanks to the rapid advancement in technology, many studies were carried out in recent years in order to improve heat transfer capacities, particularly in the systems incorporating high temperatures and heat fluxes. From this aspect, with impinging jet, the flows are commonly used as a low-cost cooling method in various applications including heat treatment of metals, metal annealing, metal sheet fabrication, cooling the gas turbine blades, turbine seals, high-density electronic chips, solar cells, internal combustion engines, drying the fabrics and paper, etc. [1, 2].

Heat transfer can be improved by making use of various methods such as fluid injection or suction, expanded surfaces, vibrating the heated surfaces, and improving the fluid characteristics. Another option is to improve the cooling effect by impinging the fluid jet cooling method. It is possible to lower the thickness of the heater surface thermal boundary layer in order to achieve a high thermal performance between the impinged fluid and the contact area. This method is designed to be a low-cost and attention-grabbing cooling method [3, 4].

Numerous experimental and theoretical studies examining the jet impingement energy transfer were carried out on different applications ranging between turbine blade cooling and fast convective heating. Several remarkable literature reviews were published [2, 5-7]. For instance, thermal performances of singular round jets, groups of round jets, individual slot (2-D zone) jets, and slot jet grids were analyzed.

As reported in the previous studies [2, 8, 9], three distinctive zones are generated by the formation of a single impinging jet from the nozzle on a flat target surface. These areas are known as the stagnation zone, free jet zone, and wall jet zone.

CFD (Computational Fluid Dynamics) is a branch of fluid mechanics that is based on numerical analysis and algorithms to solve problems that involve fluid flows.

Experimental and theoretical methods are two main approaches in engineering system design. In experimental methods, heat and flow characteristics of the produced heat sink model are experimentally determined in a wind tunnel. In theoretical methods, the heat and flow characteristics are obtained by making use of numerical solutions of the governing differential equations. Nowadays, engineers use both experimental and CFD analysis effectively [10].

In an experimental and numerical study, Shariatmadar et al. investigated the increase of the heat transfer from a flat surface by using multiple air-impinging jet slots. The effects of Reynolds number ($Re=234 - 470$), jet width size ($W=2-5$ mm), and number of slot jets on the mean Nusselt number were investigated. The researchers determined that, as the Reynolds number increased, the boundary layer along the wall became thinner around the impinging area, causing an increase in the Nusselt number. Their findings showed that the local Nu number and the Re number both increased with the increasing slot width [11].

Sharif conducted a numerical analysis on the increased heat transfer by utilizing dual oblique slot-jet impingement. Setting Reynolds number to 1000 and nozzle-to-target distance to 6 and using twin oblique slot-jet, four different angle values (45° , 60° , 75° , and 90°) and streamline and isotherm patterns (in the flow domain) were examined. The results showed that the jet angle has a considerable influence on the flow and temperature of target surfaces. Furthermore, it was also determined that the heat transfer was not adequately distributed for the impingement angles up to 60° . On the other hand, at the impingement angle of 45° , the heat transfer was reasonably distributed resulting in a decrease of approx. 36% in the overall heat transfer [7].

Caggese et al. conducted a numerical and experimental research in order to examine the increase in heat transfer of completely restricted jet impingement and the heat transfer coefficients were determined. The air jet had effects on each tow wall displayed by using the Reynolds number ($Re = 16500 - 41800$) and the jet-to-plate distance, which ranged from 0.5 to 1.5 diameter of jet. The momentum, pressure, and energy components were calculated using the second-order upwind differencing method. The highest Nusselt numbers were observed with the target surface located at a jet-to-plate distance of 1 jet diameter. The highest Nusselt numbers for the 14 impingement surface were recorded at the jet-to-target separation of $d/2$. Thus, the mean heat transfer of the target surface was approx. 45% less than that of the target surface, which was subjected to the impingement jet zones directly [12].

Yakut et al. examined the cooling efficiency by using the free jet method with nozzle on a plate having hexagonal fins. The nozzle diameter was 50 mm. Their study was carried out practically and numerically using Ansys Fluent program. Six different speeds of cooling air coming out of the nozzle were tested by using three different fin heights and different nozzle-to-target distances. Numerical predictions based on $k-\epsilon$ reliable turbulence model were in good coherence with experimental results. The Nusselt number correlations obtained from the experimental and numerical results were very close to each other and had a high accuracy rate [13].

Bozdoğan analyzed the cooling efficiency by using the free jet method with nozzle on a plate having rectangular fins. This study was carried out practically. Six different speeds of cooling air coming out of the nozzles were tested in this study using four different nozzle diameter and three different nozzle-to-target distances. Numerical predictions based on $k-\epsilon$ reliable turbulence model were in good coherence with the experimental results. The numerical results showed that the mean Nusselt number was directly proportional to the increase in Reynolds number. The Nusselt number also increased with the increasing value of the nozzle diameter. The results were explained graphically ($Nu-Re$) in his study. The Nusselt number correlations obtained from experimental had a high accuracy rate [14].

Wan et al. carried out a numerical and experimental study on the thermal fluid properties in the multiple fluid jetting cooling systems. Flat, inline pin-fin, and scattered pin-fin were the three surfaces used. Results were obtained at air Re numbers ranging from $15 \cdot 10^3$ to $35 \cdot 10^3$. The data obtained indicate that mean Nu values increased with increasing Re number. Furthermore, it was also observed that the inline pin-fin plate had the highest mean Nusselt numbers, followed by the staggering pin-fin plate and the flat plate [15].

Yousefi-Lafouraki et al. carried out numerical research on the forced convection and entropy production by utilizing a restricted slot impinging jet with Al_2O_3 -water nanofluid. Results were reported for the Reynolds numbers of 100 - 500, the jet-to-target plate spacing of 4 - 10, and the nanoparticles volume fraction of 0 - 6 %. It was determined that the local and mean Nusselt numbers increased with increasing Re number and nanoparticle focus. Furthermore, it was also shown that the thermal and frictional entropy generation increased with increasing Re number. Conversely, the local Nu number, thermodynamic performance, and entropy production were found to decrease with an increasing nozzle-to-target gap [16].

Xu et al. used air jet impingement in order to simulate heat transfer and entropy formation. A rough target surface subjected to the slot jet impingement was modeled by using a sinusoidal wave and the results were compared to those of a smooth surface. The Reynolds number used in these tests ranged between 2738 and 10952 with a jet-to-plate distance of 4 to 8 jet diameters. The heat transfer performance of the rough surface was found to be significantly higher than that of the smooth target surface. When compared to a smooth target plate, the mean heat transfer coefficient of a rough surface was up to 40% higher. In addition, it was discovered that increasing the Re number led to increases in the Nu number, entropy generated, heat transfer, and fluid friction [17].

Manca et al. carried out a numerical study on a restricted jetting hole filled with Al_2O_3 -water nanofluid in order to improve the heat transmission. Numerical simulations were performed at different

Reynolds numbers ranging between 5000 and 20000, the nanoparticles concentrations between $\phi = 0$ and 6%, and the jet-to-target plate space between 4 and 20. The authors illustrated that the highest local Nusselt number was found at the stagnation area, whereas the lowest value was found at the target plate's ending. The results showed that the highest heat transfer enhancement up to 16% was obtained at a jet-to-target gap of 10 and a volume fraction of 6%. Moreover, for all the situations, the numerical findings revealed that the required pumping power increased with increasing Reynolds number and nanoparticle concentration [18].

A numerical analysis was carried out by Vaziei and Abouali on the fluid flow and the thermal performance enhancement for Al_2O_3 -water nanofluid using jet impingement. The circular submerged and confined jet impinging on the smooth surface was considered. Nanofluid was used at two concentrations as 2.8 and 6%, with Reynolds numbers ranging between 250 and 500 and the jet-to-target space ranging between 2 and 5 jet diameters. The test results showed that the use of nanofluids can remarkably enhance the rate of heat transfer in the laminar jet. It was determined that the stagnation Nusselt number was doubled by using a 6% volume fraction at the jet-to-plate spacing of 2 jet diameters. In addition, the tests revealed that the Nu number and friction coefficient increased with increasing nanoparticle volume fraction [19].

Beriache et al. carried out a numerical study on the heat transfer and fluid flow of the impingement flow with the mini-channel heat sink. The authors examined the hydraulic and thermal characteristics of the heat sink under forced convection cooling conditions. The governing equations of momentum, continuity, and energy were solved numerically by using the finite-difference method. The Reynolds numbers of cooling air at range between 200 and 1000. It was observed that increasing Reynolds number leads to the removal of heat from the heat sinks gradually [20].

II. MATERIAL and METHOD

In the present study, heat transfer and fluid flow characteristics were numerically determined for optimized rectangular finned heat sinks by using impingement jet flow. Moreover, ANSYS k- ϵ model options were used for numerical analysis. The model was preferred because it yielded convergent results in previous studies comparing the experimental and numerical results [10, 13, 21, 22]. The analyses were performed for three different nozzle diameters ($D=50, 63, \text{ and } 75\text{mm}$), 4 different flow velocities, and three different heat fluxes ($q=2222, 3333, 4444 \text{ W/m}^2$) for the heat sink. Given the CFD results, Nu-Re graphics were presented. Geometry and mesh of rectangular finned heat sinks, which were optimized using the Taguchi experimental $L_{18}(2^1 \cdot 3^7)$ design method [23] with impingement jet flow, were created.

The heat sink optimized in the previous studies was used in the numerical analyses [24]. The heat sinks were optimized using Taguchi experimental design method. The optimization criterion used for the Nusselt number was “the bigger the better”. Calculating the Nusselt number by making use of the nozzle diameter, the optimized results were found to be the fin width of 15 mm, fin angle of 30° , fin height of 100 mm, spanwise distance between fins of 20 mm, streamwise distance between fins of 10 mm, spanwise distance between slices of 20 mm, streamwise distances between slices of 10 mm and flow velocity of 9 m/sec. (See Figs. 1 and 2; Table 1).

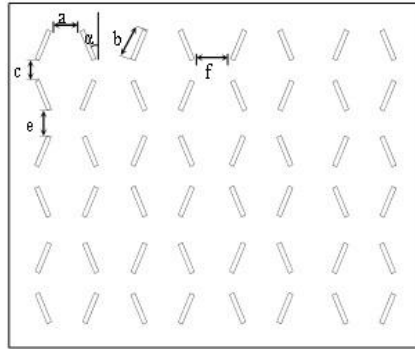


Figure 1. The general characteristics of the heat sink.

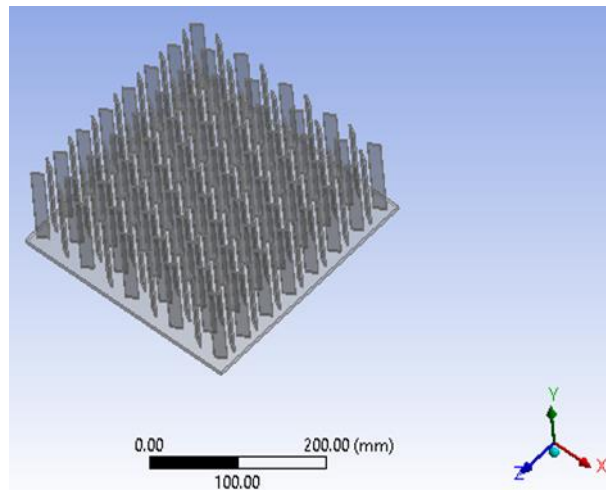


Figure 2. The perspective view of the optimized rectangular pin fin heat sink.

Table 1. Dimensions of the rectangular-finned heat sink.

Parameter	Description	Value
a	The horizontal distance between fins	10 mm
b	Fin width	15 mm
c	The vertical distance between fins	20 mm
e	The vertical distance between slices	20 mm
f	The horizontal distance between slices	10 mm
t	The thickness of the base heat sink	5 mm
h_k	Fin height	100 mm
α	Fin angle	30°

Since the analyses were performed in symmetrical geometry, the symmetrical solution was preferred. The numerical mesh was first created on the mesh page without any changes in order to gain information before creating the digital mesh. After the mesh was knitted, the mesh quality was determined. Aspect ratio, skewness, and the number of elements that can be checked from the section were determined by using the optimum values obtained from the other knitted digital mesh. In the “boundary conditions” menu, calculations were made for different speed ranges. The inlet temperature of the air was set to be 293 K and heat flux value to be 2222 W/m², 3333 W/m², and 4444 W/m². For the insulated surfaces, the thermal option was determined as heat-flux, the heat flux value was entered as 0 and the surface was defined as insulated in the program. Analyses were made with the assumption

that an average problem would converge in 3000 iterations. After the problems were solved, it was tested if the problem converged (diverged) and it was determined if there was turbulence. Moreover, the stability state conditions of the heat sink were tested thoroughly.

A. COMPUTATIONAL ANALYSIS

Continuity, turbulent momentum, and turbulent energy equations were solved using ANSYS Fluent under suitable boundary conditions for three-dimensional incompressible flow. Conservation equations for turbulent flow in Cartesian coordinates can be written as follows:

Continuity equation

$$\frac{\partial \rho}{\partial t} + \nabla \cdot (\rho V) = 0 \quad (1)$$

Navier-Stokes equation

$$\rho \frac{\partial V}{\partial t} + \rho V \cdot \nabla V = -\nabla P + \mu \nabla^2 V \quad (2)$$

The energy equation

$$\rho \bar{\mu}_j \frac{\partial \bar{T}}{\partial x_j} = -\frac{\partial}{\partial x_j} \left[\left(\frac{\mu_l}{\sigma_l} + \frac{\mu_t}{\sigma_t} \right) \frac{\partial \bar{T}}{\partial x_j} \right] \quad (3)$$

The momentum equation

$$\rho \bar{\mu}_j \frac{\partial \bar{\mu}_i}{\partial x_j} = -\frac{\partial \bar{p}}{\partial x_i} + \frac{\partial}{\partial x_j} \left[\mu_t \left(\frac{\partial \bar{\mu}_i}{\partial x_j} + \frac{\partial \bar{\mu}_j}{\partial x_i} \right) \right] \quad (4)$$

The governing equation for solid

$$\frac{\partial}{\partial x_i} \left[k_s \frac{\partial T}{\partial x_i} \right] = 0 \quad (5)$$

Where k_s refers to the thermal conductivity of solid (heat sink).

Reynolds number equation

$$Re = \frac{\rho U_{avg} D_h}{\mu} \quad (6)$$

Where, D_h refers to the hydraulic diameter, U_{avg} to the average velocity, ρ to the density, and μ to the dynamic viscosity of the fluid

$$U_{avg} = 0.817 U_o \quad (7)$$

Where, U_o refers to the maximum velocity of air jet.

Average convection coefficient

$$h_{avg} = \frac{Q}{A_s(T_{s,avg} - T_j)} \quad (8)$$

Where, Q refers to the heat flux, A_s to the surface area of the heat sink, $T_{s,avg}$ to the average temperature of the heat sink, and T_j to the jet air temperature.

$$A_s = WL + 2Nh_k(t + b) \quad (9)$$

Where, W refers to the width of the base plate on which the blades are placed, L to the length of the base plate, h_k to the height of the blades, t to the thickness of the blades, b to the width of fin, and N to the total number of blades on the plate.

Average Nusselt number

$$Nu = \frac{h_{avg}d}{k} \quad (10)$$

Where, d refers to the inner diameter of the nozzle, k to the thermal conductivity of the fluid, and h_{avg} to the average convection coefficient.

III. RESULTS and DISCUSSION

In the present study, impingement jet cooling was numerically analyzed. Nozzle diameters and impingement jet and heat flux velocities are among the most effective parameters on the heat transfer of finned surfaces. It was determined that the two most efficient parameters on heat transfer of finned heat sinks were the fin height (h) and diameter of nozzle (d) or flow rate (v ; Re), respectively. The distance between nozzle and heat sink is also a very important parameter. However, $h/d=1$ distance was used in previous experimental studies and it was observed that the best heat transfer was achieved with $h/d=1$ [14, 24, 25]. Therefore, numerical analyses were performed for optimum rectangular pin-fin heat sink at four different impingement jet velocities (10, 12, 14, and 16 m/s), three different nozzle diameters ($D=50, 63, \text{ and } 75$ mm), and three different heat fluxes ($Q=2222, 3333, \text{ and } 4444$ W/m^2) at fixed dimensionless nozzle-heat sink distance ($h/d=1$). Using the CFD results achieved, Nu-Re graphics were created.

Given the results of numerical analysis, it can be seen that the Nusselt Number increases with increasing Reynolds Number for all cases. However, the ratio of increase differs depending on nozzle diameter, jetting air velocity, and heat flux value. An increase in the nozzle diameter leads to an increase in the Nusselt number. The best thermal performance was achieved at the largest diameter ($D=75$ mm), followed by the diameter of (63 mm), whereas the smallest diameter (50 mm) yielded the worst thermal performance for each heat flux value. The highest Nusselt number was found with the heat flux of 4444 W/m^2 , diameter of 75 mm, and $U_o=16$ m/s.

A. VARIATION OF NUSSULT NUMBER BY THE REYNOLDS NUMBER

A. 1. Comparison of Numerical Results for ($q=2222$ W/m^2)

The Nusselt number increases with the increasing Reynolds Number. Moreover, an increase in the nozzle diameter leads to an increase in the Nusselt number, too. The consequences of Nu numbers varying with the Re number by the nozzle diameter ($D=50$ mm, 63 mm, and 75 mm) are illustrated in Figure 3.

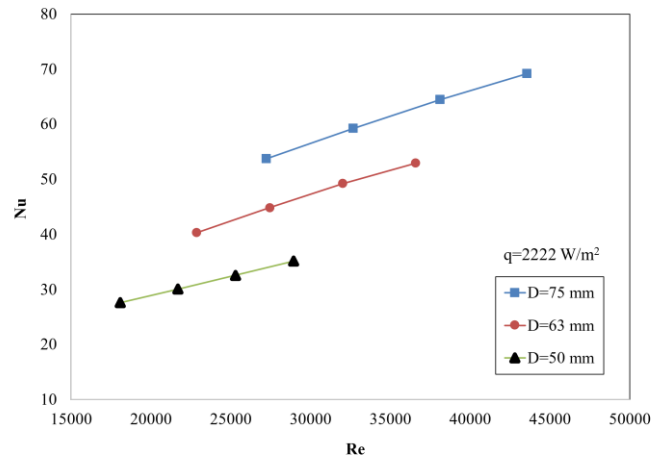


Figure 3. Numerical analysis of $(Nu-Re)$ at $q=2222 \text{ W/m}^2$.

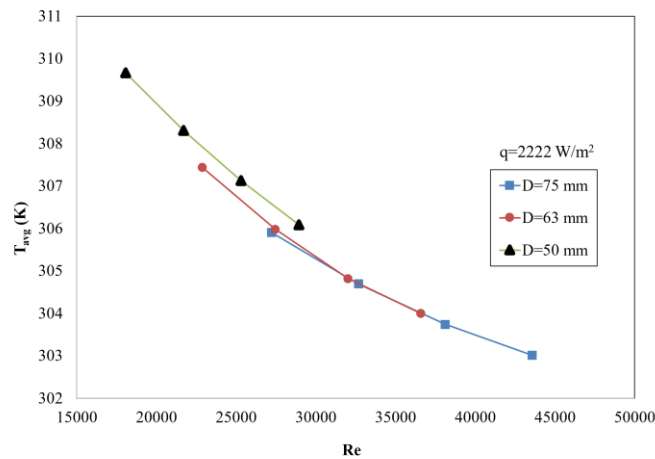


Figure 4. Numerical analysis of average temperature at $q=2222 \text{ W/m}^2$.

An increase of 7.3% to 10.4% was observed in Nu numbers between successive speed levels with increasing velocity in the rectangular fin plate for the nozzle diameter 75 mm, 7.5% to 11.2% for the nozzle diameter 63 mm, and 7.9% to 8.9% for the nozzle diameter 50 mm. It was calculated that the total Nusselt number increased by 26.5% for the nozzle diameter 75 mm, 28.5% for the nozzle diameter 63 mm, and 25.2% for the nozzle diameter 50 mm in the range of maximum and minimum velocities. For the heat sink, the Nu number at $D=75 \text{ mm}$ improved by 30.8% compared to its value at $D=63 \text{ mm}$, and the value at $D=63 \text{ mm}$ was 50.5% higher than the value of $D=50 \text{ mm}$ at the maximum velocity.

A. 2. Comparison of Numerical Results for $(q=3333 \text{ W/m}^2)$

The Nusselt number increases in parallel with the increasing Reynolds Number. An increase in nozzle diameter leads to an increase in the Nusselt number. The consequences of Nu numbers varying with the Re number by the nozzle diameter ($D=50 \text{ mm}$, 63 mm , and 75 mm) are illustrated in Figure 5.

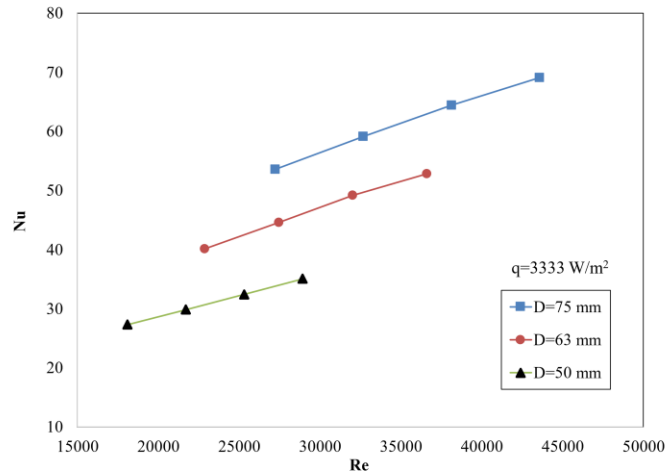


Figure 5. Numerical analysis of $(Nu-Re)$ at $q=3333 \text{ W/m}^2$.

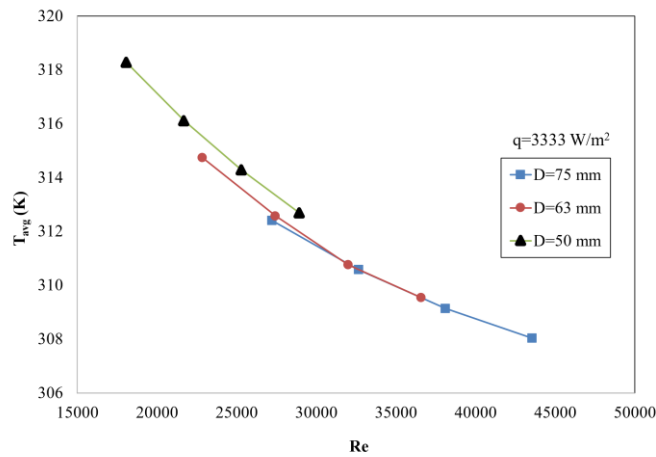


Figure 6. Numerical analysis of average temperature at $q=3333 \text{ W/m}^2$.

Given the results of numerical analyses, an increase of 7.3% to 10.4% was observed in Nu numbers between successive speed levels with increasing velocity in the rectangular fin plate for the nozzle diameter 75 mm, 7.4% to 11.1% for the nozzle diameter 63 mm, and 8.1% to 9.3% for the nozzle diameter 50 mm. It was calculated that the total Nusselt Number increased by 26.7% for the nozzle diameter 75 mm, 28.7% for the nozzle diameter of 63 mm, and 26.1% for the nozzle diameter 50 mm in the range of maximum and minimum velocities. For the heat sink, the Nu number at D=75 mm improved by 30.9% compared to its value at D=63 mm, and the value at D=63 mm is 50.6% higher than the value of D=50 mm at the maximum velocity.

A. 3. Comparison of Numerical Results for $(q=4444 \text{ W/m}^2)$

The Nusselt number increases with the increasing Reynolds Number. Increasing the nozzle diameter leads to an increase in the Nusselt number. The consequences of Nu numbers varying with the Re number by the nozzle diameter (D=50 mm, 63 mm, and 75 mm) are presented in Figure 7.

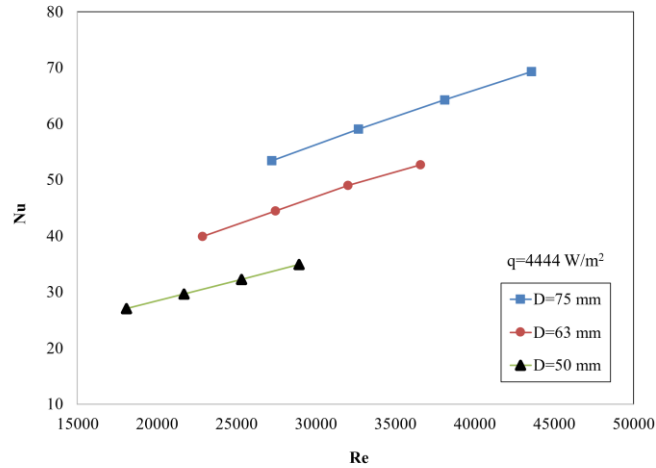


Figure 7. Numerical analysis of $(Nu-Re)$ at $q=4444 \text{ W/m}^2$

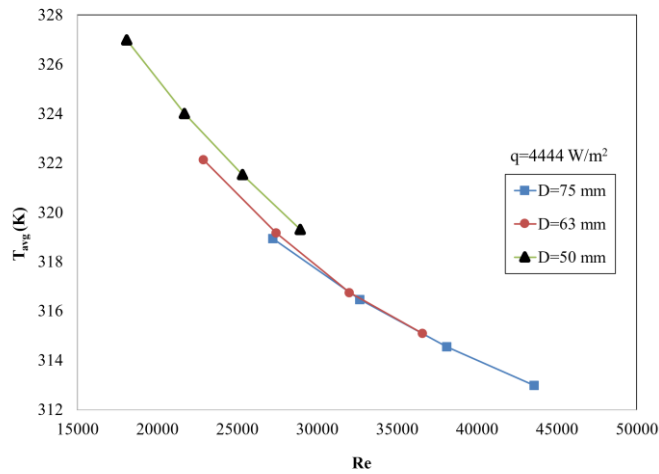


Figure 8. Numerical analysis of average temperature at $q=4444 \text{ W/m}^2$.

Given the numerical analysis results, an increase by 7.8% to 10.5% was observed in Nu numbers between successive speed levels with increasing velocity in the rectangular fin plate for the nozzle diameter 75 mm, 7.5% to 11.4% for the nozzle diameter 63 mm, and 8.5% to 9.6% for the nozzle diameter of 50 mm. It was calculated that the total Nusselt Number increased by 27.2% for the nozzle diameter of 75 mm, 29.1% for the nozzle diameter of 63 mm, and 26.8% for the nozzle diameter of 50 mm in the range of maximum and minimum velocities. For the heat sink, the Nu number at D=75 mm was improved by 31.6% compared to its value at D=63 mm, and the value at the D=63 mm was found to be higher by 50.7% in comparison to the value of D=50 mm at the maximum velocity.

VI. CONCLUSION

Together with the significant advancement in technology, improving the efficiency of devices and equipment, which led to an increase in the heat generated by them and hinders the development process, draws more attention among researchers. Therefore, researchers' interest in the technology of jetting with nozzles, which has been used in many fields thanks to its high performance and speed of processing distinguishing it from the other methods, also increased. The present study focused on examining several variables affecting the performance of this method. The fluid flow characteristics, which are represented by the air used to cool the optimized rectangular finned heat sink, were studied by using the impingement jet-cooling technique. The numerical analysis method was used in

experiments and then the results were compared to the experimental results obtained under the same working conditions and variables. The variables were air velocity ($U_o=10, 12, 14, \text{ and } 16 \text{ m/s}$), and change in the nozzle diameter ($D=75, 63, \text{ and } 50 \text{ mm}$), and change in the heat flux ($q=2222, 3333, \text{ and } 4444 \text{ W/m}^2$). It was aimed to achieve the highest thermal performance for these variables. The results presented in the previous sections can be summarized as follows:

- The Nusselt number increases with increasing Reynolds Number for all cases. However, the rate of increase varies depending on nozzle diameter and jetting air velocity.
- Increasing the nozzle's diameter leads to an increase in the Nusselt number. The best thermal performance was achieved at the largest diameter ($D=75 \text{ mm}$), followed by the diameter of 63 mm , whereas the smallest diameter (50 mm) yielded the worst thermal performance.
- The highest Nusselt number was found at the heat flux of 4444 W/m^2 , diameter of 75 mm , and $U_o=16 \text{ m/s}$.
- Given the numerical results, the highest thermal performance was achieved by changing the nozzle diameter from 50 to 75 mm ; it led to an increase in the Nusselt number by $94.6\% - 99.5\%$ at $U_o=10-16 \text{ m/s}$, respectively. On the other hand, changing the nozzle diameter from 50 to 75 mm , the thermal performance increased and the increase in Nusselt number was found to be $46 - 52\%$. However, the nozzle diameter was changed from 63 to 75 mm , the Nusselt number increased by $31\% - 33.7\%$.
- The increase in the velocity of jetting air resulted in an increase in the Nusselt number for all cases. But the rate of increase varied depending on the nozzle diameters. Comparing the Nusselt numbers by the maximum and minimum velocities and heat fluxes examined, it was determined that velocity increased with an increase in the number of Nusselt by $(26.5\%-27.2\%)$ at the diameter of 75 mm , while the increase in Nusselt number was found to be $28.5\%-29.1\%$ for the diameter of 63 mm . On the other hand, the diameter of 50 mm yielded the lowest increase in the Nusselt number ($25.2\% - 26.8\%$) with an increase in the velocity.

NOMENCLATURE

NOMENCLATURE			
A	Area (m^2)	Nu	Nusselt number
a	The horizontal distance between fins (mm)	Re	Reynolds number
b	Width of fin (m)	T	Temperature (K)
c_p	Pressure coefficient (J/kgK)	t	Thicknesses of fin (m)
c	The vertical distance between fins (mm)	U	Velocity (m/s)
d	Nozzle diameter (m)	W	Width of the base plate (m)
e	The vertical distance between slices (mm)	μ	Dinamic Viscosity (kg/ms)
f	The horizontal distance between slices (mm)	ρ	Density (kg/m^3)
h	Convection coefficient ($\text{W/m}^2\text{K}$)	Subscripts	
h_k	Height of fin (m)	ave	Average
h/d	Dimensionless distance between nozzle-target surface	h	Hidrolic
k	Conduction coefficient (W/mK)	s	Surface
L	Lenght of the base plate (m)	tot	Total
N	Number of fins		

V. REFERENCES

- [1] A. Basaran and F. Selimefendigil, “Numerical study of heat transfer due to twinjets impingement onto an isothermal moving plate”, *Mathematical and Computational Applications*, vol. 18, no.3, pp. 340-350, 2013.
- [2] R. Viskanta, “Heat transfer to impinging isothermal gas and flame jets”, *Experimental Thermal and Fluid Science*, vol. 6, no. 2, pp. 111-134, 1993.
- [3] X. Liu and J. H. Lienhard, “Extremely high heat fluxes beneath impinging liquid jets”, *ASME Journal of Heat Transfer*, vol. 115, no. 2, pp. 472-476, 1993.
- [4] J. H. Lienhard V and J. Haderler, “High heat flux cooling by liquid jet-array modules”, *Chemical Engineering & Technology: Industrial Chemistry-Plant Equipment-Process Engineering-Biotechnology*, vol. 22, no. 11, pp. 967-970, 1999.
- [5] T. H. Park, H. G. Choi, J. Y. Yoo and S. J. Kim, “Streamline upwind numerical simulation of two-dimensional confined impinging slot jets”, *International Journal of Heat and Mass Transfer*, vol. 46, no. 2, pp. 251-262, 2003.
- [6] M. Molana, and S. Banoooni, “Investigation of heat transfer processes involved liquid impingement jets: A review”, *Brazilian Journal of Chemical Engineering*, vol. 30, no. 3, pp. 413-435, 2013.
- [7] M. A. Sharif, “Heat transfer from an isothermally heated flat surface due to twin oblique slot-jet impingement”, *Procedia Engineering*, vol. 56, pp. 544-550, 2013.
- [8] O. Al-aqal, “Heat transfer distributions on the walls of a narrow channel with jet impingement and cross-flow”, Ph.D. dissertation, Department of Mechanical Engineering, University of Pittsburgh, Pennsylvania, USA, 2003.
- [9] P. S. Penumadu and A. G. Rao, “Numerical investigations of heat transfer and pressure drop characteristics in multiple jet impingement system”, *Applied Thermal Engineering*, vol. 110, pp. 1511-1524, 2017.
- [10] K. Guresci, F. Yesildal, A. Karabey, R. Yakut and K. Yakut, “Numerical analysis with experimental comparison in duct flow using optimized heat sinks”, *Journal of Radiation Research and Applied Sciences*, vol. 11, no. 2, pp. 116-123, 2018.
- [11] H. Shariatmadar, A. Momeni, A. Karimi, and M. Ashjaee, “Heat transfer characteristics of laminar slot jet arrays impinging on a constant target surface temperature”, *Applied Thermal Engineering*, vol. 76, pp. 252-260, 2015.
- [12] O. Caggese, G. Gnaegi, G. Hannema, A. Terzis and P. Ott, “Experimental and numerical investigation of a fully confined impingement round jet”, *International Journal of Heat and Mass Transfer*, vol. 65, pp. 873-882, 2013.
- [13] R. Yakut, K. Yakut, F. Yeşildal and A. Karabey, “Experimental and numerical investigations of impingement air jet for a heat sink”, *Procedia Engineering*, vol. 157, pp. 3-12, 2016.
- [14] D. Bozdogan, “Experimental and numerical analysis of heat and flow characteristics with impingement jet for optimized rectangular finned heat sinks”, M.S. thesis, Institute of Natural and Applied Sciences, Van Yuzuncu Yil University, Van, Turkey, 2020.

- [15] C. Wan, Y. Rao and P. Chen, “Numerical predictions of jet impingement heat transfer on square pin-fin roughened plates”, *Applied Thermal Engineering*, vol. 80, pp. 301-309, 2015.
- [16] B. Yousefi-Lafouraki, A. Ramiar and A. A. Ranjbar, “Numerical investigation of laminar forced convection and entropy generation of nanofluid in a confined impinging slot jet using two-phase mixture model”, *Iranian Journal of Science and Technology, Transactions of Mechanical Engineering*, vol. 43, no. 1, pp. 165-179, 2019.
- [17] P. Xu, A. P. Sasmito, S. Qiu, A. S. Mujumdar, L. Xu and L. Geng, “Heat transfer and entropy generation in air jet impingement on a model rough surface”, *International Communications in Heat and Mass Transfer*, vol. 72, pp. 48-56, 2016.
- [18] O. Manca, P. Mesolella, S. Nardini and D. Ricci, “Numerical study of a confined slot impinging jet with nanofluids”, *Nanoscale Research Letters*, vol. 6, no. 1, pp. 1-16, 2011.
- [19] P. Vaziei and O. Abouali, “Numerical study of fluid flow and heat transfer for Al₂O₃-water nanofluid impinging jet”, *7th International Conference on Nanochannels, Microchannels, and Minichannels*, (ISBN No. 978-0-7918-4349-9), 2009, pp. 977-984.
- [20] M. Beriache, A. Bettahar, H. Naji, L. Loukarfi, and L. M. Saïdia, “Fluid flow and thermal characteristics of a mini channel heat sink with impinging airflow”, *Arabian Journal for Science and Engineering*, vol. 37, no.8, pp. 2243-2254, 2012.
- [21] A. Yeşilyurt, “Experimental and numerical investigation of cooling with multiple air jet impingement”, M.S. thesis, Graduate School of Natural and Applied Sciences, Atatürk University, Erzurum, Turkey, 2019.
- [22] R. A. A. Al-Ani, “Numerical analysis of heat and flow characteristics with impingement cooling jet for optimized rectangular finned heat sink”, M.S. thesis, Institute of Natural and Applied Sciences, Van Yüzüncü Yıl University, Van, Turkey, 2021.
- [23] P. Ross, *Taguchi Techniques For Quality Engineering*, McGraw-Hill, Singapore, 1989.
- [24] A. Karabey, “Determination of heat and flow characteristics of impingement jet for heat sink”, M.S. thesis, Graduate School of Natural and Applied Sciences, Atatürk University, Erzurum, Turkey, 2010.
- [25] N. Yıldız, “Investigation of heat and flow characteristic with impingement jet for optimized hexagonal finned heat sinks”, M.S. thesis, Graduate School of Natural and Applied Sciences, Atatürk University, Erzurum, Turkey, 2012.